

Influence of speed fluctuation on Cepstrum

Frédéric Bonnardot¹

¹Univ Lyon, UJM Saint Etienne, LASPI, EA 3059
F-42334, IUT de Roanne, France.
{frederic.bonnardot}@univ-st-etienne.fr

Abstract

This paper deals with the influence of speed fluctuations (non-stationary signal) on the cepstrum. Due to the non-stationarity, a time-quefreny representation is also used to study the evolution of the cepstral content. Illustrations were made by using gears signal by SAFRAN from the Surveillance 8 contests.

1 Introduction

Vibratory analysis is a very popular non-intrusive tool to perform diagnostic of rotating machinery. Nevertheless, the effect of rotation speed on the vibration signals became significant when the speed is non-stationary. In this case, instantaneous speed could be measured by using a tachometer signal and used to take account the speed for diagnostics. The rotating machine instantaneous speed provided by the tacho is also a very useful information. It could be sensitive to mechanical faults [1] and be used for diagnostics. It is also requested for computed order tracking [2].

Since a tachometer speed signal is not always available, instantaneous speed has to be estimated from other signals like the accelerometric signal. Some instantaneous speed extraction methods are described in the MSSP Special Issue on Instantaneous Angular Speed (IAS) Processing and Angular Applications [3] and [4]. These methods use analytic signal, parametric approach, ...

Another approach based on cepstrum was proposed in the Surveillance 8 Contest [4]. A cepstrum (echo detector) [5, 6] is used to estimate the instantaneous speed. This method is derived from an cepstral order tracking method presented (only in French) in [7]. Unfortunately, the cepstrum is known to be sensitive to speed fluctuations.

In this paper it is proposed to study the influence of speed fluctuations on the cepstrum. A first part recalls the classic cepstrum properties and studies the influence of speed fluctuations. In the second part, a time quefreny-representation is introduced and speed fluctuation influence is discussed by using some synthetic signals. Next some illustrations are made on real signals.

2 Cepstrum properties

Cepstrum has many applications [9] (detection of periodic components, diagnosis, modal analysis, ...). This paper is focused on detection of periodical components. Application is made on a civil aircraft engine gearbox. One application could be instantaneous period (and speed) estimation. This part explains how cepstrum could be used.

2.1 Definition

In this paper, the word cepstrum refers to power cepstrum as defined [8] by:

$$cep_{x(t)}(\tau) = \mathcal{F}^{-1}[\ln|X(f)|] \quad (1)$$

where $X(f)$ is the Fourier Transform of the signal $x(t)$, \mathcal{F}^{-1} is the Inverse Fourier Transform, and, \ln the neperian logarithm. The variable τ is homogenous to a time and is named quefreny.

2.2 Properties

Calculation to explain theoretically the results of the cepstrum on gearbox signals can be found in [6]. Some results of this paper are recalled here.

The accelerometric signal associated with a gearbox can be viewed as a repetition of a series of periodic patterns $p_k(t)$. A periodic pattern at period a_k can be interpreted as a convolution of a single pattern with a Dirac comb of period a_k . Let's consider that the gearbox can be modelled in an area small enough to neglect speed fluctuations as:

$$x(t) = \left[\sum_{k=1}^M p_k(t) * em_{a_k} \right] * h_{imp}(t) = x_w(t) * h_{imp}(t) \quad (2)$$

$$em_{a_k} = \sum_{n=0}^{n-1} \delta_{n,a_k} \quad (3)$$

where

- δ_t is the Dirac delta function delayed of t ,
- $p_k(t)$ is the pattern associated with the gear k ,
- em_{a_k} is multiple echo terms to repeat the pattern at period a_k ,
- $h_{imp}(t)$ is the impulse response of the mechanical structure,
- $*$ is the convolution product.

The term $p_k(t)$ is considered to have a constant Fourier transform of modulus P_k in [6] (i.e. to have similar property of white noise). It means that the term $x_w(t)$ could be interpreted as a whitened form of the signal without the contribution of the mechanical structure response.

1. The cepstrum transform a convolution product into an addition:

$$cep_{x(t)}(\tau) = cep_{x_w(t)}(\tau) + cep_{h_{imp}(t)}(\tau) \quad (4)$$

2. Oppenheim and Schaffer in [8] studied the impact of transfer function for digitised signal and show that for :

$$H(z) = \frac{B \prod_{i=1}^{M_i} (1 - a_i z^{-1}) \prod_{i=1}^{M_0} (1 - b_i z)}{\prod_{i=1}^{N_i} (1 - c_i z^{-1}) \prod_{i=1}^{N_0} (1 - d_i z)}, \quad (5)$$

the cepstrum is

$$cep_{h(n)}(n) = \ln(B), \quad \text{for } n=0 \quad (6)$$

$$cep_{h(n)}(n) = -\sum_i \frac{a_i^n}{n} + \sum_i \frac{c_i^n}{n}, \quad \text{for } n>0 \quad (7)$$

$$cep_{h(n)}(n) = \sum_i \frac{b_i^{-n}}{n} - \sum_i \frac{d_i^{-n}}{n}, \quad \text{for } n<0 \quad (8)$$

$$(9)$$

where c_i and a_i are the pole and zeros inside the unit circle and d_i and b_i are the pole and zeros outside the unit circle. This result shows that the cepstrum of transfer function is rather present at the beginning of the cepstrum due to the term of $1/n$.

3. According to [6], the cepstrum of the term $x_w(t)$ is composed of M positive and decreasing combs with a step a_k .

$$cep_{x_w(t)}(\tau) = \sum_{k=1}^M \left[\sum_{n \in \mathbb{Z}^*} \frac{1 - (1 - P_k)^n}{2|n|} \delta_{n,a_k} \right] \quad (10)$$

The shape in comb of $x_w(t)$ cepstrum is totally different from the one associated with $h_{imp}(t)$ cepstrum. Therefore, it is possible to visually separate the two contributions.

4. It is shown in [6] that if an additive noise is present in $x(t)$, the amplitude of the combs decreases and particularly the first peak.

For a gearbox, the cepstrum is expected to produce rharmonics associated with the shaft rotations. Since the cepstrum transforms a convolution into an addition, the part of the cepstrum associated to the Dirac comb em_{ak} is uncoupled with the part associated to the pattern $p_k(t)$ and the impulse response $h_{imp}(t)$.

An example of cepstrum coming from a gearbox is presented in Figure 1. The black lines indicates times multiples of 4 ms and red lines times multiples of 5.5 ms . Two combs with periods of 4 ms and 5.5 ms clearly appear in the cepstrum. These two period are linked with two mechanical rotating frequencies. These combs can be clearly distinguished from the rest of the cepstrum that contains elements linked with impulse response $h_{imp}(t)$. With an exception for the first and second peak, the peaks amplitude decrease when the quefrequency increase.

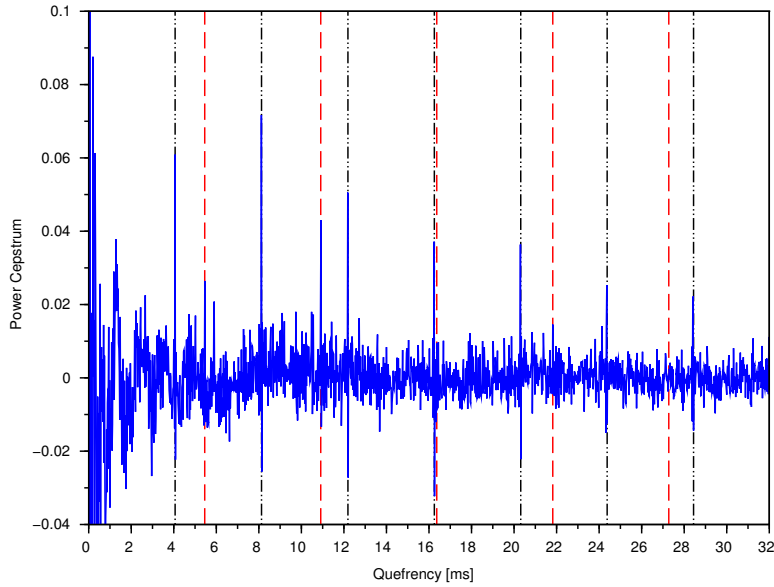


Figure 1: Cepstrum example

These properties are established by considering a constant rotation speed zone. In the next section, the effect of the period fluctuation is studied.

2.3 Effect of period (or speed) fluctuation

Response of a cepstrum to simple and multiple echoes with a decreasing amplitude has been studied in [10]. In this paper, we are interested in the case of echoes of the same amplitude, and, with a fluctuation in the localisation of the echoes due to speed fluctuations.

2.3.1 2 echoes with shift

To explore the effect of the period fluctuation, the following model of 2 echoes of shift a with a fluctuation Δ is introduced in this paper:

$$e_{a,\Delta} = \delta_0 + \delta_a + \delta_{2a+\Delta}. \quad (11)$$

The Fourier Transform (\mathcal{F}) of $e_{a,\Delta}$ is:

$$\mathcal{F}(e_{a,\Delta}) = 1 + e^{-2\pi jfa} + e^{-2\pi jf(2a+\Delta)} \text{ with } j^2 = -1. \quad (12)$$

Its modulus, lower than 3 is:

$$\begin{aligned} |\mathcal{F}(e_{a,\Delta})| &= \sqrt{3+2\{\cos(2\pi fa) + \cos[2\pi f(a+\Delta)] + \cos[2\pi f(2a+\Delta)]\}} \\ &= \frac{3}{\sqrt{2}} \sqrt{1 + \frac{4}{9} \left\{ \cos(2\pi fa) + \cos[2\pi f(a+\Delta)] + \cos[2\pi f(2a+\Delta)] - \frac{3}{4} \right\}} \end{aligned}$$

By using Taylor expansion of \ln , the energy cepstrum is:

$$ceps_{e_{a,\Delta}}(\tau) = \ln\left(\frac{3}{\sqrt{2}}\right) \cdot \delta_0 + \frac{\mathcal{F}^{-1}[Y(f)]}{2} \quad (13)$$

where

\mathcal{F}^{-1} is the inverse Fourier Transform,

$$\begin{aligned} Y(f) &= \sum_{n \in \mathbb{N}^*} \frac{(-1)^{n-1} \cdot 4^n}{n \cdot 9^n} \left\{ \cos(2\pi fa) + \cos[2\pi f(a+\Delta)] + \cos[2\pi f(2a+\Delta)] - \frac{3}{4} \right\}^n \\ &= \sum_{n \in \mathbb{N}^*} \frac{(-1)^{n-1} \cdot 4^n}{n \cdot 9^n} \sum_{i+j+k+l=n} \binom{n}{i,j,k,l} \cos^i(2\pi fa) \cdot \cos^j[2\pi f(a+\Delta)] \cdot \cos^k[2\pi f(2a+\Delta)] \cdot \left(-\frac{3}{4}\right)^l \end{aligned}$$

and

$$\binom{n}{i,j,k,l} = \frac{n!}{i!j!k!l!}. \quad (14)$$

The Inverse Fourier Transform of $Y(f)$ is:

$$y(\tau) = \sum_{n \in \mathbb{N}^*} \frac{(-1)^{n-1} \cdot 4^n}{n \cdot 9^n} \sum_{i+j+k+l=n} \binom{n}{i,j,k,l} \left(-\frac{3}{4}\right)^l \left[\left(\frac{\delta_{-a} + \delta_a}{2}\right)^{*i} * \left(\frac{\delta_{-a-\Delta} + \delta_{a+\Delta}}{2}\right)^{*j} * \left(\frac{\delta_{-2a-\Delta} + \delta_{2a+\Delta}}{2}\right)^{*k} \right]$$

where $*$ is the convolution product, a^{*n} means a convoluted n times, and $a^{*0} = \delta_0$.

Let us define $\binom{i}{m} = \frac{i!}{m!(i-m)!}$ and the function $z(i) = \begin{cases} 0 & \text{for } i = 0 \\ 1 & \text{for } i \neq 0 \end{cases}$.

Since

$$\left(\frac{\delta_{-a} + \delta_a}{2}\right)^{*i} = \frac{1}{2^i} \sum_{m=0}^i \binom{i}{m} \delta_{(i-2m)a.z(i)} \quad (15)$$

it is possible to simplify $y(\tau)$ to:

$$\begin{aligned} y(\tau) &= \sum_{n \in \mathbb{N}^*} \frac{(-1)^{n-1} \cdot 2^n}{n \cdot 9^n} \sum_{i+j+k+l=n} \binom{n}{i,j,k,l} \left(-\frac{3}{2}\right)^l \sum_{p=0}^i \sum_{q=0}^j \sum_{r=0}^k \binom{i}{p} \binom{j}{q} \binom{k}{r} \delta_s \\ s &= a[i+j+2k-2pz(i)-2qz(j)-4rz(k)] + \Delta[j+k-2qz(j)-2rz(k)] \end{aligned}$$

The energy cepstrum is finally:

$$ceps_{e_{a,\Delta}}(\tau) = \ln\left(\frac{3}{\sqrt{2}}\right) \cdot \delta_0 + \frac{y(\tau)}{2} \quad (16)$$

In order to explain this expression easily, a simulation is made. The figure 2 shows the Test signal $e_{a,\Delta}$, its cepstrum computed numerically (echo shift of $a = 1\ 000$ samples, fluctuations of $\Delta = 66$ samples, signal length of 100 000 samples), and a cepstrum enlargement. Theoretical values computed with equation (16) by considering a Taylor expansion of order $n = 2$, $n = 5$, $n = 10$ are given with different colours on the enlargement. The peak at quefrency 0 is outside the scale (it is not exploited here).

By looking at the figure, the following observations are made:

1. Two peaks are found at quefrency a and $a + \Delta$. There are side bands of decreasing amplitude spaced from Δ near these two peaks.

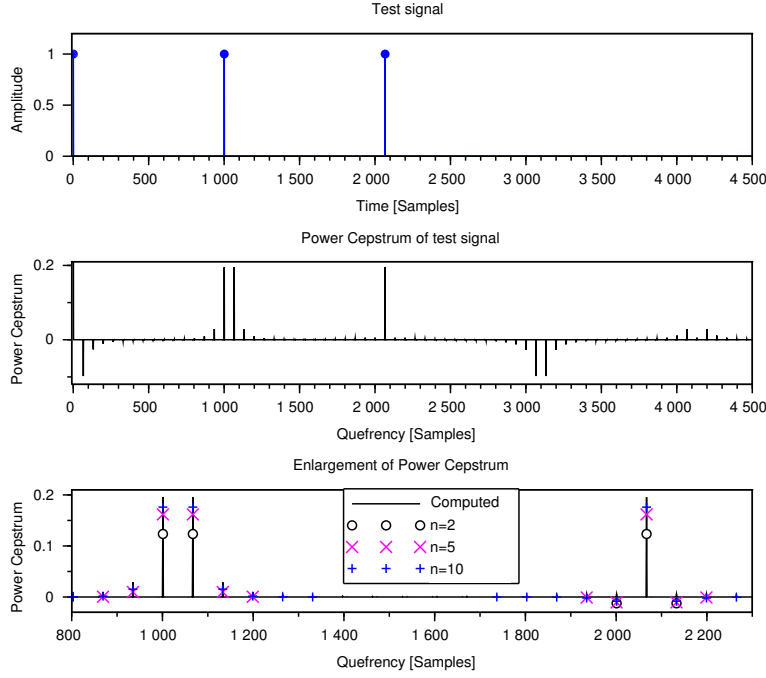


Figure 2: Cepstrum of 2 echoes of shift a with fluctuation ($a=1000$, $\Delta = 66$)

2. One peak is present at queffrency $2a + \Delta$. The one at $2a$ is just a side band with a low amplitude.
3. Negative peaks indicates the fluctuation at queffrency Δ . They explains the absence of positive echo at $3.a + \Delta$.
4. Take account the side bands in equation (16) involves using a high Taylor expansion order.
5. The higher the Taylor expansion order is, the closest the peaks amplitude are.
6. Observing higher queffrencies show that rharmonics of the followed peaks exist and that they decrease rapidly.
7. Without fluctuations ($\Delta = 0$), the peaks amplitude at queffrency a and $a + \Delta$ are replaced by a peak of double amplitude (sum of the amplitude of the two latter).

By using a Taylor expansion of order $n = 1$ of equation (16) the expression $y(\tau)$ became:

$$y(\tau) = \frac{2}{9} \left[\delta_a + \delta_{-a} + \delta_{a+\Delta} + \delta_{-a-\Delta} + \delta_{2a+\Delta} + \delta_{-2a-\Delta} - \frac{3}{2} \delta_0 \right] \quad (17)$$

In this equation, contributions at queffrencies a , $a + \Delta$, $2a + \Delta$ clearly appears. It can be noticed that no term exists at queffrency $2a$.

When considering a higher Taylor expansion order :

- a term at queffrency $2a$ is introduced for higher Taylor order, but, at a smaller amplitude,
- negative terms could appear for even value of $n + l$ (for example at queffrency $3a$),
- more sidebands are generated (see the expression of s) but with a smaller value due to the coefficients.

2.3.2 Multiple echoes with shift

In case of multiple echoes with shifts, the model of equation (11) is generalised into multiple echoes of shift a with a fluctuation Δ_i :

$$em_{a,\Delta_i,M} = \delta_0 + \sum_{i=1}^M \delta_{i.a+\Delta_i}. \quad (18)$$

Its Fourier Transform is:

$$\mathcal{F}(em_{a,\Delta_i,M}) = 1 + \sum_{i=1}^M e^{-2\pi j f (ia + \Delta_i)} \quad (19)$$

$$= A_M - j.B_M \quad (20)$$

with:

$$A_M = 1 + \sum_{i=1}^M \cos[2\pi f (ia + \Delta_i)] \text{ and}$$

$$B_M = \sum_{i=1}^M \sin[2\pi f (ia + \Delta_i)].$$

Its scarred modulus is:

$$|\mathcal{F}(em_{a,\Delta_i,M})|^2 = A_M^2 + B_M^2, \quad (21)$$

with the following recurrence:

$$A_M^2 + B_M^2 = A_{M-1}^2 + B_{M-1}^2 + 1 + 2 \cos[2\pi f (Ma + \Delta_M)] \quad (22)$$

$$+ 2 \sum_{i=1}^{M-1} \cos\{2\pi f [a(M-i) + \Delta_M - \Delta_i]\} \quad (23)$$

$$A_0 = 1 \quad (24)$$

$$B_0 = 0. \quad (25)$$

Its modulus, lower than $M+1$ is:

$$|\mathcal{F}(em_{a,\Delta_i,M})| = \frac{M+1}{\sqrt{2}} \cdot \sqrt{1 + 2 \cdot \frac{A_M^2 + B_M^2}{(M+1)^2} - 1}. \quad (26)$$

By using Taylor expansion of \ln , the energy cepstrum is:

$$ceps_{em_{a,\Delta_i,M}}(\tau) = \ln\left(\frac{M+1}{\sqrt{2}}\right) \cdot \delta_0 + \frac{\mathcal{F}^{-1}[Z(f)]}{2} \quad (27)$$

where

$$Z(f) = \sum_{n \in \mathbb{N}^*} \frac{(-1)^{n-1}}{n} \left[2 \cdot \frac{A_M^2 + B_M^2}{(M+1)^2} - 1 \right]^n. \quad (28)$$

Since $Z(f)$ is composed only of cosine wave and constant term, its contribution in the cepstrum will be a set of Dirac at cosine frequencies (including null frequency). By considering a Taylor expansion at order $n = 1$ (for simplicity), and considering the recurrence defined at equation (22) it is possible to find the Dirac position associated by using the algorithm 1.

Figure 3 shows a test signal with 4 echoes with a period of 1 000 samples and a fluctuation $\Delta = [0; 66; -130; 103]$. Corresponding quefrequencies computed according to algorithm 1 are presented in the table 1. The colours used in this table is linked with the one used in the cepstrum on figure 3.

By looking at figure 3, the following observation can be made:

1. Considering only the order $n = 1$ in equation (28) enables to compute the most energetic quefrequencies.
2. There are Dirac in cepstrum at the same location than the Dirac in the test signal: $i.a + \Delta_i$. These Dirac have the same Power.

Input: Number of echoes M , shifts Δ_i , period a
Result: List of quefrequencies Q
if $M=1$ **then**
 | $Q \leftarrow [a + \Delta_1]$;
else
 | $Q \leftarrow$ quefrequencies associated with $M - 1$ echoes with fluctuation Δ_i ;
 | $Q \leftarrow [Q; 0]$;
 | $Q \leftarrow [Q; Ma + \Delta_M]$;
 for $i \leftarrow 1$ **to** $M - 1$ **do**
 | $Q \leftarrow [Q; a(M - i) + \Delta_M - \Delta_i]$;
 end
end
return Q ;

Algorithm 1: Quefrequencies associated with M echoes with fluctuation Δ_i

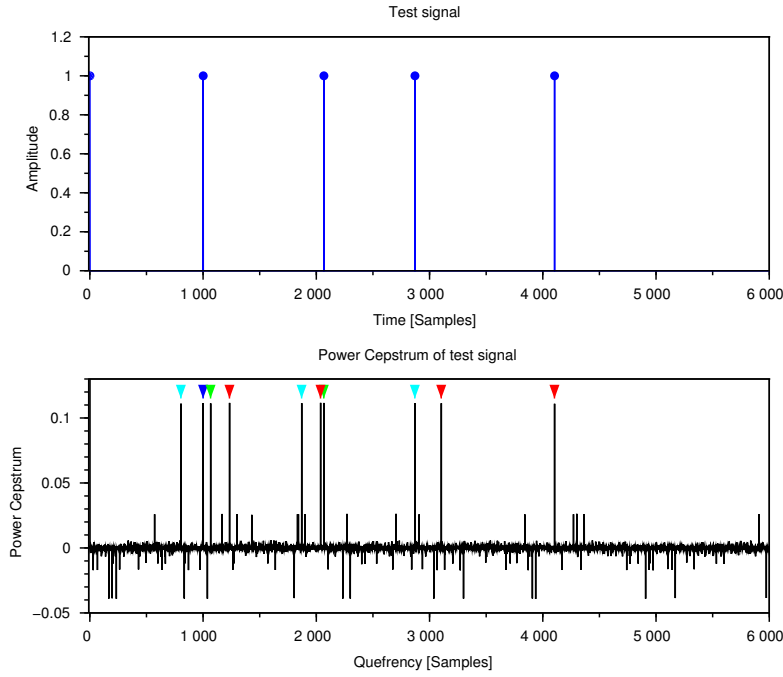


Figure 3: Cepstrum of 4 echoes of shift a with fluctuation ($a=1000$, $\Delta = [0; 66; -130; 103]$)

M	Quefrequencies added at M^{th} step	Numerical Values
1	$a + \Delta_1$	1 000
2	$2a + \Delta_2; a + \Delta_2 - \Delta_1$	2 066 ; 1 066
3	$3a + \Delta_3; 2a + \Delta_3 - \Delta_1; a + \Delta_3 - \Delta_2$	2 870 ; 1 870 ; 804
4	$4a + \Delta_4; 3a + \Delta_4 - \Delta_1; 2a + \Delta_4 - \Delta_2; a + \Delta_4 - \Delta_3$	4 103 ; 3 103 ; 2 037 ; 1 233

Table 1: Quefrequencies associated to 4 echoes ($a = 1000$; $\Delta = [0; 66; -130; 103]$)

3. There is $M - i$ Diracs around the quefrequency associated to the i^{th} echo (i.e. 3 Diracs near quefrequency 1 000, 2 near quefrequency 2 066, ...).
4. The set of distances between these Diracs and $i.a$ are $\{\Delta_p - \Delta_q\}$ where $p - q = i$ and $1 + i \leq p \leq M$.

The fluctuation values used in this example is "high" in comparison with the shift a . For smaller fluctuations values, the peaks will be closer to quefrequencies $a, 2.a, \dots$. For the quefrequency $i.a$, if the set of fluctuations $\{\Delta_p - \Delta_q\}$ (where $p - q = i$ and $1 + i \leq p \leq M$) is lower than 1, the fluctuation is not detectable by the cepstrum at quefrequency $i.a$ and only one main peak should appear. Therefore, a tracking quefrequency is possible for small fluctuations.

The next section will introduce the time-quefrequency representation that enables to compute a series a cepstrum against the time and to perform period tracking. It also shows its sensitivity to period variation (quadratic form).

3 Time-quefrequency representation

3.1 Definition

Let define the time-quefrequency representation at instant t , quefrequency τ , with a window length w by:

$$TQR_{x(t)}(t; \tau; w) = cep_{x(m).rect_w(m-t)}(\tau), \quad (29)$$

where $rect_w(t)$ is a rectangular window of length w defined by

$$rect_w(t) = \begin{cases} 1 & \text{for } 0 \leq t < w, \\ 0 & \text{outside.} \end{cases} \quad (30)$$

3.2 Test signal

In order to simulate a fluctuation (increasing period), a test signal is generated. To create this test signal a series of $K = 150$ peaks distances position d_k is defined by:

$$d_k = 100.0 + 0.1k \quad \text{for } 1 \leq k \leq 50 \quad (31)$$

$$d_k = d_{50} + 0.4(k - 50) \quad \text{for } 51 \leq k \leq 100 \quad (32)$$

$$d_k = d_{50} + 0.4(k - 50) + 0.02(k - 100)^2 \quad \text{for } 101 \leq k \leq 150. \quad (33)$$

This test signal is composed of three parts. A linearly decreasing period with a step of 1. Another linearly decreasing period with a higher step of 4, and, a quadratic form of decreasing period.

The peak position can be obtained by:

$$p_1 = 1 \quad (34)$$

$$p_{k+1} = p_k + d_k \quad (35)$$

In order to generate peaks at non-integer position, an 10 times up-sampled signal $tfq(n)$ is generated by setting to amplitude 1 the set of elements at positions $\{round(10.p_k)\}$ and leaving the other values to 0. The test signal $tq(n)$ is obtained by decimating by a factor 10 the signal $tfq(n)$. The decimation enables to have peaks at non-integer positions in $tq(n)$.

3.3 Test signal cepstrum

In order to understand the time quefrequency representation of the test signal, a particular instant t is considered. Depending on the rectangular windows length w , at time t , the term $wx(t; w) = x(m).rect_w(m-t)$ in equation (29) contains the peaks at instants p_K to p_{K+I} where p_K is the first element greater than t and p_{K+I} is the last element lower than $t + w$.

Since the cepstrum is sensitive to distance between peaks, it is interesting to compute the distance $dp_{K,\alpha}$ between the peak at instant p_K and another peak at instant $p_{K+\alpha}$. If the term d_k is identified as a polynomial form at order 2:

$$d_k = q + r.k + s.k^2 \quad (36)$$

the distance is:

$$dp_{K,\alpha} = p_{K+\alpha} - p_K \quad (37)$$

$$= \sum_{\beta=0}^{\alpha-1} d_{K+\beta} \quad (38)$$

$$= (\alpha - 1)p_K + \frac{\alpha(\alpha - 1)}{2}(r + 2.K.s) + \frac{\alpha(\alpha - 1)(2\alpha - 1)}{6}s. \quad (39)$$

The term $wx(t;w)$ could be interpreted as a series I echoes of the peak at position p_K . By analogy with equation (18) of the multiple echo with shifts, it could be considered that the shift a and fluctuation Δ_i are:

$$a = p_K \quad (40)$$

$$\Delta_i = \frac{i(i-1)}{2}(r + 2.K.s) + \frac{i(i-1)(2i-1)}{6}s \quad (41)$$

$$dp_{K,\alpha} = (\alpha - 1)a + \Delta_\alpha. \quad (42)$$

At the difference of the multiple echo shift, the first peak instant is p_K and not 0. Since the cepstrum is sensitive to echoes, there is no change in cepstrum peak position.

According to the section 2.3.2, cepstrum position there are peaks in the cepstrum at quefrecies:

$$\{p_K + \Delta_{i+1} - \Delta_i\}_{i=0..I-1} = \{p_K + i(r + 2K.s) + s.i^2\}_{i=0..I-1} \quad (43)$$

and rharmonics:

$$\{2.p_K + \Delta_{i+2} - \Delta_i\}_{i=0..I-2} = \left\{ 2.p_K + (2i+1)(r + 2.K.s) + s.\frac{5i^2 + 3i + 1}{3} \right\}_{i=0..I-2} \quad (44)$$

$$\{3.p_K + \Delta_{i+3} - \Delta_i\}_{i=0..I-3} \quad (45)$$

...

For the 100 first values of k in the test signal, d_k is linear ($s = 0$). The previous peak location in cepstrum becomes:

$$\{p_K + \Delta_{i+1} - \Delta_i\}_{i=0..I-1} = \{p_K + i.r\}_{i=0..I-1} \quad (46)$$

$$\{2.p_K + \Delta_{i+2} - \Delta_i\}_{i=0..I-2} = \{2.p_K + (2i+1).r\}_{i=0..I-2} \quad (47)$$

$$\{3.p_K + \Delta_{i+3} - \Delta_i\}_{i=0..I-3} \quad (48)$$

...

By looking at these equations, the following observations can be made:

1. There is a peak on cepstrum at quefrecy p_K . So, the cepstrum can be used to measure the instantaneous frequency p_K .
2. For a linear form of d_k (i.e. $s = 0$) at the right of quefrecy p_K there is a series of $I - 1$ peaks distant each other from r . This distance is the same whatever the index K and depends only on factor r .
3. For a quadratic form of d_k , this distance depends on K : it grows against the time t in the time-quefrecy representation.

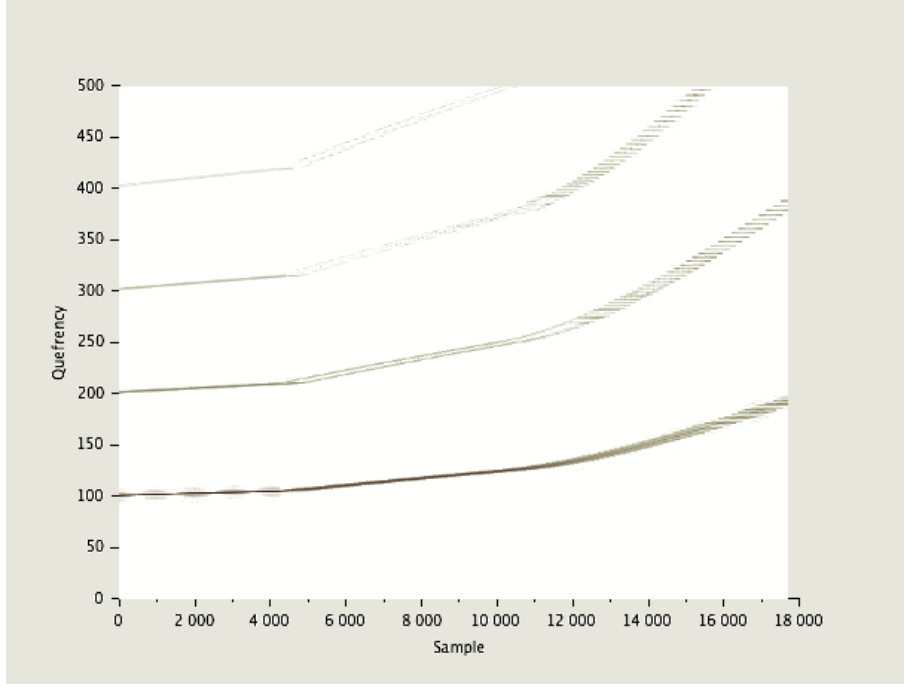


Figure 4: Time Quefrequency Representation - Log Scale - Quefrequency scale divided by 10 (due to decimation)

4. The number of peaks $I + 1$ inside this window depends on the size w of the window. If the window length is small enough to have the quantity $I(r + 2K.s) + s.I^2$ of equations (43) lower than a sample, the additional peak created near p_K will not be visible.
5. The peak associated with the rharmonics of order 2 in the cepstrum are at quefrequency $2.p_K + \varepsilon$ with $\varepsilon = r + 2.K.s + s/3$. For $s = 0$, the introduced bias ε will be depend on the value of r . According to remark 2, the importance of r could be evaluated in the cepstrum.
6. The section 2.3.2 considers a Taylor expansion of order 1. This discussion concerns the associated peaks. Lower peaks could appear on the cepstrum as shown in figure 3.

3.4 Simulation

The figure 4 shows a time quefrequency representation of $tq(n)$ with a window of length $w = 1000$ samples. Slices of time frequency representation at the beginning, middle, and ending of the sequence are presented on figure 5 (linear scale).

Theses figures lead to the following observation:

1. At sample $t = 0$, peak at quefrequency 100 and rharmonics $\{200, 300, 400\}$ can be identified. The gray level (i.e. peaks amplitude) decrease with the rharmonic rank.
2. The 3 areas can also be identified : a slow slope (0.1) between samples 0 and 5000, a higher slope (0.4) between samples 5000 and 10000, and, a quadratic period increase after.
3. According to equation (46) and (47), some peaks should appear after the fundamental p_K and its rharmonics at a distance proportional to the slope r . Since the slope is low in the first area, this distance is lower than quefrequency resolution, and, theses peaks are merged with the one at p_k and its rharmonics. This is illustrated by the top of the figure 6. This figure shows the histogram of the distances d_k inside the windows of length w (see equation 30) at sample 1000 ($k = 11$ to $k = 20$). On the left, the step between classes of 0.01 enable to distinguish each distance. When this step takes the value of 1 only 2 classes represents the distances distribution like in the cepstrum.

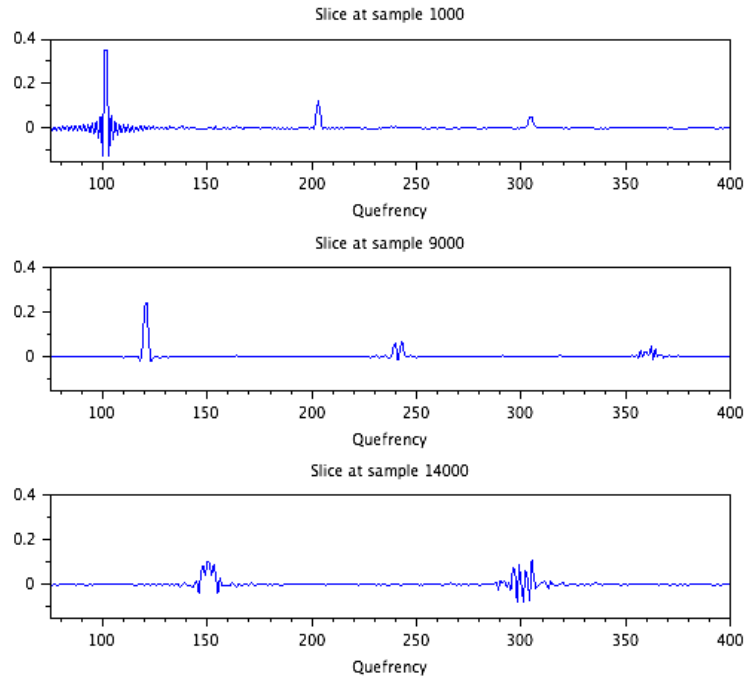


Figure 5: Slices of Time Quefrency Representation - Linear Scale

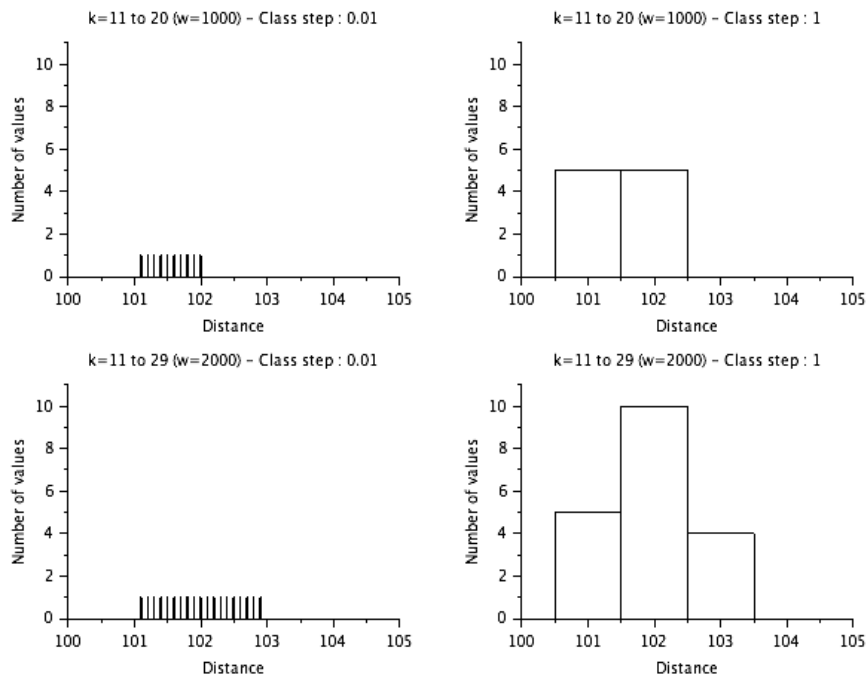


Figure 6: Histogram of d_k at sample 1000

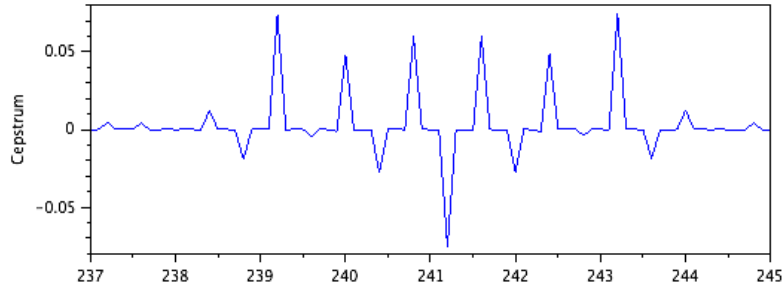


Figure 7: Slice of Time Quefrency Representation at sample 9000 without decimation

4. In the second area the slope increase. It leads to a larger distribution of d_k in the histogram and a larger peak in the cepstrum. The time quefrency slices on figure 5 effectively show that the cepstrum peak associated with the fundamental becomes larger between the first and second area. Its amplitude also becomes smaller.
5. In the second area, a second peak appears near rharmonics of rank 2. The distance between the second peak and the rharmonics increases with the rharmonic order as indicates equation (47). Following the same reasoning as the previous case, the variable d_k should be replaced by $d_k + d_{k+1}$ for histogram computation. Nevertheless, the factor $r = 0.4$ is too small to justify the apparition of these peaks. In order to investigate a cepstrum computed without decimation (i.e. a sample rate 10 times higher) is presented on figure 7. Here, a series of peaks spaced by 0.8 (i.e. two times 0.4 because of rharmonic of rank 2) clearly appears. But another series of negative peaks also appears between. These peaks can be linked with the ones on figure 3 (they do not appear in our model because an approximation at order 1 is used). When a cepstrum is computed with less precision like in figure 5, the decimation effect combine positive and negative peaks and creates two peaks.
6. In the last area, the slope constantly increase (quadratic evolution of the distance). Therefore, the distance between peaks become high enough to distinguish many peaks nears rharmonics. The distance between these peaks also increases (slowly) against the time (like the slope). The number of peaks associated to a rharmonic depends on the number of peaks I contained inside the windowed version of the signal as indicated by equations (43) and next ones. The evolution of the signal in this area looks like a step. It is simply because the cepstrum evolves when a new peak appears inside a window or another one disappears.
7. With the window of length $w = 1000$ samples (figure 5), there is 10 peaks at sample 1000. The distance between peaks increases of $r = 0.1$ samples at each new peak (i.e. a difference of 1 samples between the distance of the first two peaks and the last two peaks contained in the window). It explains the thickness of 2 samples of the peak near quefrency 100. When window length is doubled $w = 2000$ on figure 8, there is 21 peaks, and a difference of 2.1 samples. It explains that the peak is larger. The cost of enlargement is a lower amplitude. Therefore, the size of the windows should be chosen such as the variation between the distance of the peaks should not be too important (i.e. the amplitude of cepstrum peak should not be too low).

4 Application on SAFRAN signals

The concept of Time Quefrency analysis was illustrated on data issued from SAFRAN Contest at Conference Surveillance 8 [11] described in [4]. These data sampled at $F_s = 50 \text{ kHz}$ (sampling period of $20 \mu\text{s}$) come for a civil aircraft engine with a gearbox (multistage) and are recorded with a non-stationary rotation speed. The cepstrum on a stationary area was presented on the figure 1. Many quefrencies associated with the gearbox shafts appears.

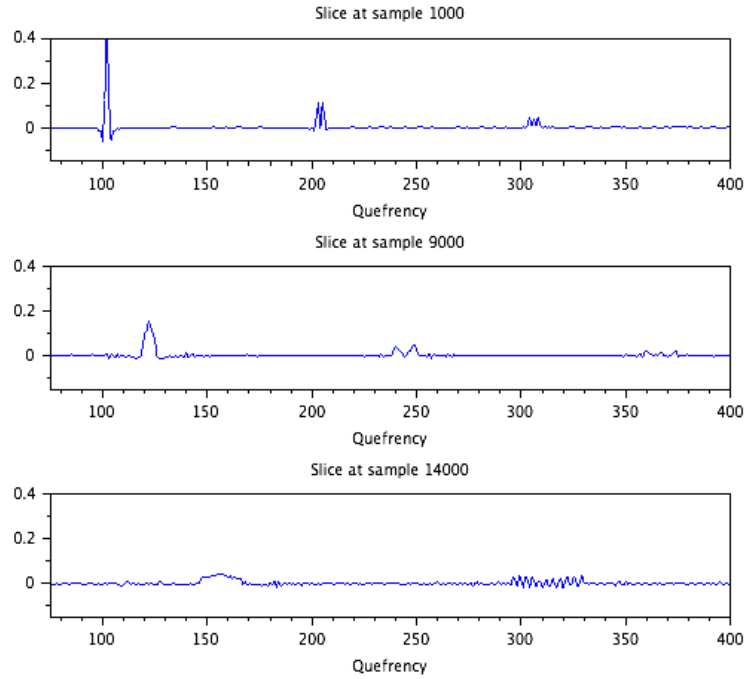


Figure 8: Slices of Time Quefrency Representation - Linear Scale - Twice window size

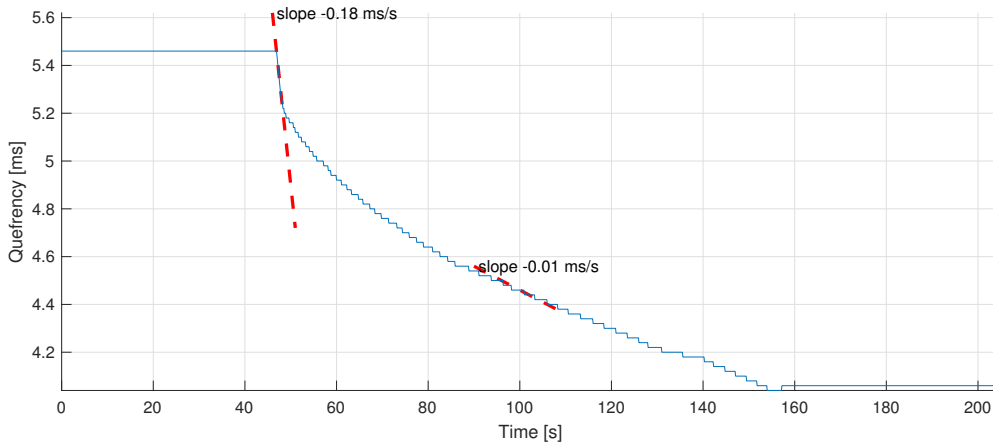


Figure 9: Tracking of quefrency beginning at 5.5 ms

By tracking the quefrency near 5.5 ms against the time it is possible to obtain the instantaneous period variation against the time as shown in the figure 9.

The area at 47 s with a slope of -0.18 ms/s and 100 s with a slope of -0.01 ms/s was selected in order to see the influence of the speed variation on the cepstrum.

The previous part shows that period fluctuation creates additional peaks near the fundamental quefrency. If the period fluctuation or quefrency resolution is low, these additional peaks are combined and appears as a large one. The number of additional peaks depends on the size of the windows.

Figures 10 and 11 shows the time-quefrency representation computed respectively $t = 47 \text{ s}$ and $t = 100 \text{ s}$. The time is fixed for each graph and the influence of the windows size w on the cepstrum is studied. Each figure is enlarged around the peak at 5.4 ms (quefrency became 4.4 ms at $t=100 \text{ s}$). The bottom of this figure shows the evolution of the maximum of the cepstrum (in the displayed area) against the window size.

For a small window size in the figure 10, the peak at 5.4 ms is sharp. It becomes larger when the window size increases.

A slope of -0.18 ms/s means an instantaneous period reduction of $0.18 \cdot 10^{-3} \times 5 \cdot 10^{-3} = 1 \mu\text{s}$ at each cycle. A window size of 0.1 s contains 20 cycles of 5 ms. It means that the cepstrum contains 20

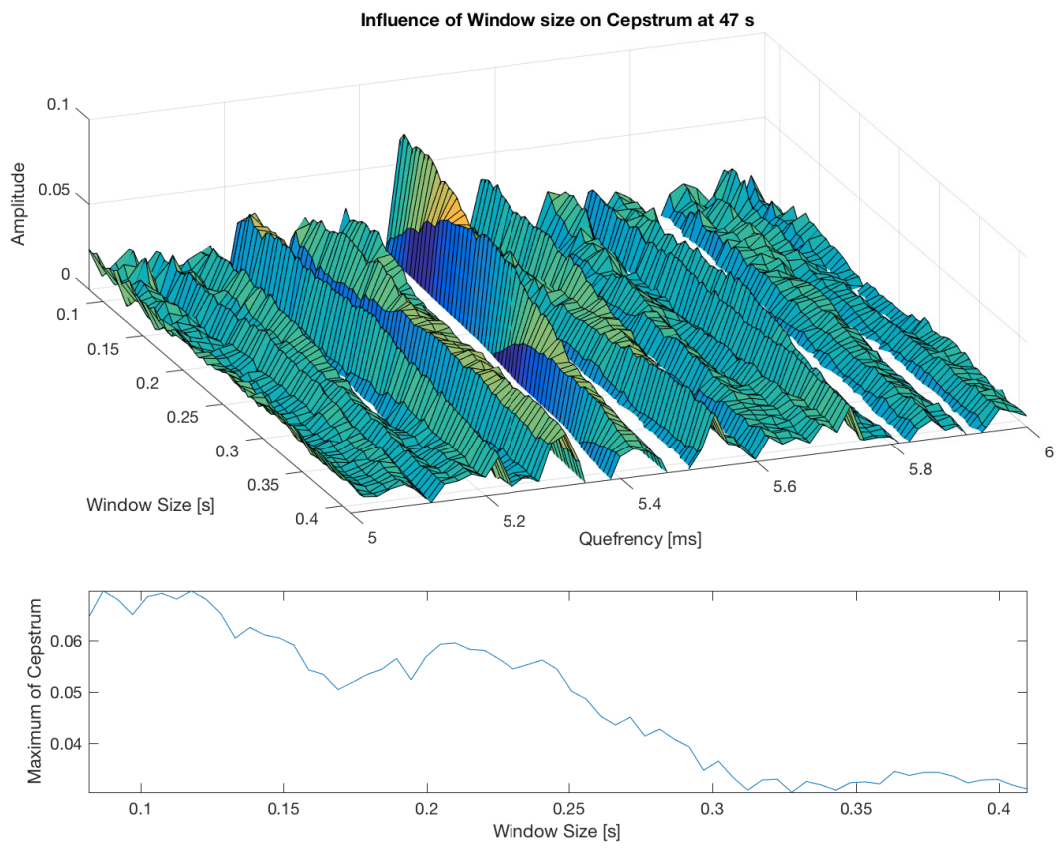


Figure 10: Influence of Window size at $t=47$ s

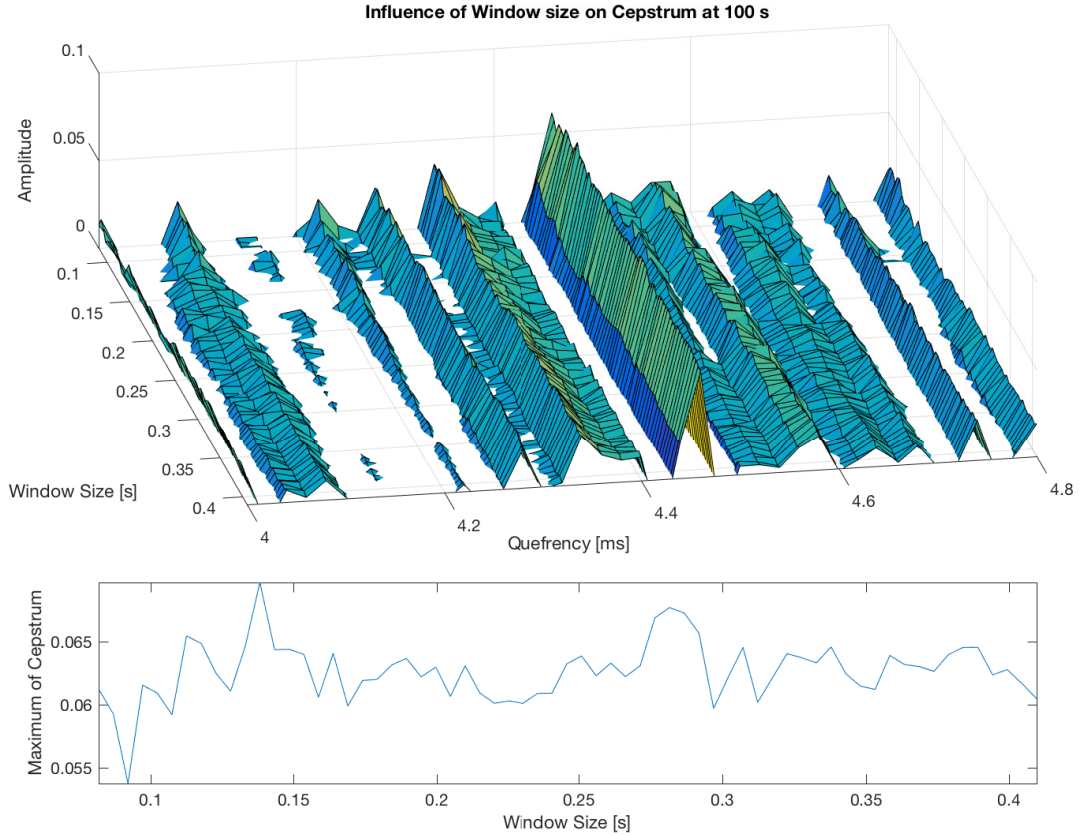


Figure 11: Influence of Window size at $t=100s$

peaks spaced by $1 \mu s$ near the quefreny $5.4 ms$. Since the sampling period of $20 \mu s$ is lower than $1 \mu s$, these peaks appear as one.

When the windows size grows, the number of cycles inside the window also grows. At $t = 0.4 s$ there is 80 cycles that corresponds to a width of $80 \mu s$ (i.e. 4 samples) that can be observed on the figure.

When the peak becomes larger, this amplitude becomes lower : the same energy is concentrated into a wider area.

On the figure 11, the slope is 20 times lower. Therefore, the influence of the period fluctuation does not affect the width of the cepstrum with a window size lower than $0.4 s$.

It can be concluded that the size of the cepstrum windows should take account the slope of the instantaneous period : rapid change means lowest windows size. Due to the result of figure 10 a windows length of $w = 0.08 s$ was chosen for time quefreny computation. Time Quefreny Representation 12 is shown on figure 12 .

The instantaneous period profile can be easily recognised on this figure by following at the fundamental quefreny of the shaft at $5 ms$ and its rharmonics. Other rharmonics that does not evolve with the same profile could also be seen.

This Time Quefreny Representation can be used to extract the instantaneous period profile by making a time quefreny tracking as explained in [4]. The instantaneous profile obtained after time quefreny tracking is shown on figure 9.

5 Conclusion

This paper has recalled some results of the cepstrum for stationary signal (i.e. no speed fluctuation). Next, it extends these results in the case of the period fluctuation and illustrates its effects. It was

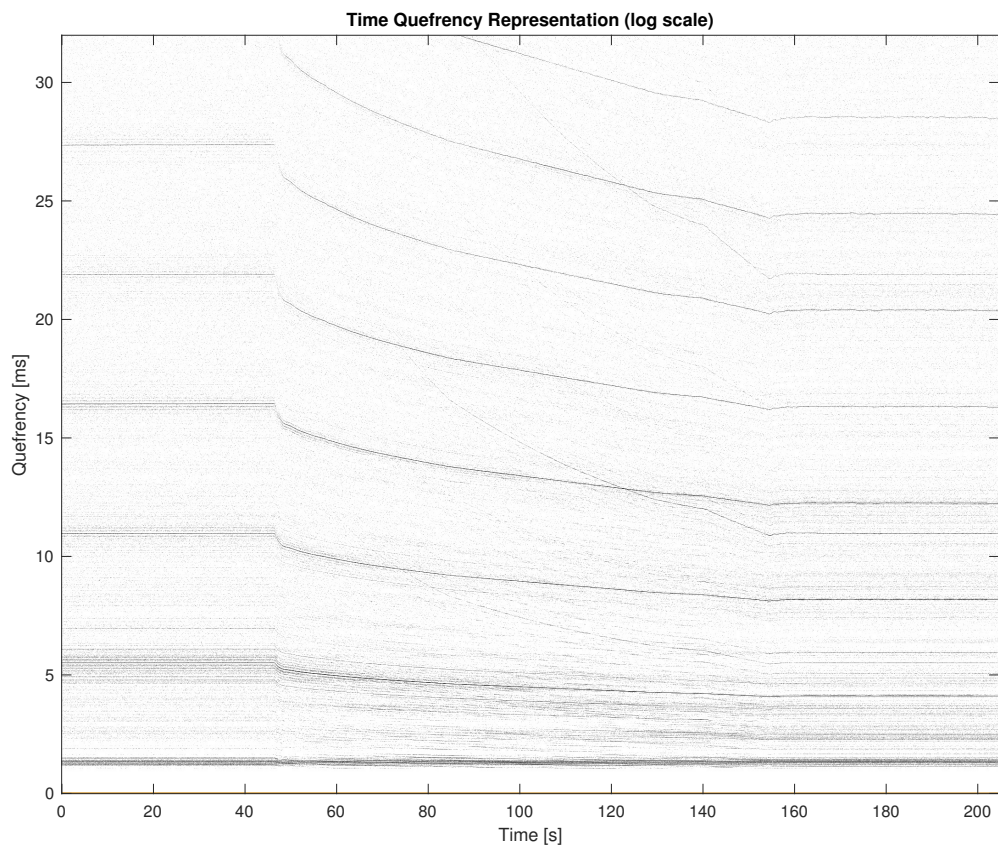


Figure 12: Time Quefrency Representation

shown that the peak at each quefrequency is split in many peaks distant from the fluctuation. Time Quefrequency representation was also proposed to see the evolution of the period fluctuation against the time. Time Quefrequency Representation was applied on synthetic and real signal. It was shown that the window length should be small enough to produce sharp peaks at quefrequency of interest.

References

- [1] L. Renaudin, F. Bonnardot, O. Musy, J.B. Doray, and D. Rémond. Natural roller bearing fault detection by angular measurement of true instantaneous angular speed. *Mechanical Systems and Signal Processing*, 24(7):1998 – 2011, 2010. Special Issue: ISMA 2010.
- [2] F. Bonnardot, M. El Badaoui, R.B. Randall, J. Danière, and F. Guillet. Use of the acceleration signal of a gearbox in order to perform angular resampling (with limited speed fluctuation). *Mechanical Systems and Signal Processing*, 19(4):766 – 785, 2005.
- [3] D. Rémond, J. Antoni, and R.B. Randall. Editorial for the special issue on instantaneous angular speed (ias) processing and angular applications. *Mechanical Systems and Signal Processing*, 44(1–2):1 – 4, 2014. Special Issue on Instantaneous Angular Speed (IAS) Processing and Angular Applications.
- [4] Jérôme Antoni, Julien Griffaton, Hugo André, Luis David Avendaño-Valencia, Frédéric Bonnardot, Oscar Cardona-Morales, German Castellanos-Dominguez, Alessandro Paolo Daga, Quentin Leclère, Cristián Molina Vicuña, David Quezada Acuña, Agusmian Partogi Ompusunggu, and Edgar F. Sierra-Alonso. Feedback on the surveillance 8 challenge: Vibration-based diagnosis of a safran aircraft engine. *Mechanical Systems and Signal Processing*, pages –, 2017.
- [5] B.P. Bogert, M.J.R. Healy, and J.W. Tukey. The frequency analysis of time series of echoes: cepstrum pseudo-autocovariance cross-cepstrum and saphe cracking. In *Proceedings of the Symposium on Time Series Analysis*, pages 209–243, 1963.
- [6] M.El Badaoui, F. Guillet, and J. Danière. New applications of the real cepstrum to gear signals, including definition of a robust fault indicator. *Mechanical Systems and Signal Processing*, 18(5):1031 – 1046, 2004.
- [7] F. Bonnardot, J. Danière, M. El Badaoui, and F. Guillet. Ré-échantillonnage synchrone cepstral. Nice, 6-7 May 2004.
- [8] A.V. Oppenheim and R.W. Schaffer. Discrete-time signal processing. 1989.
- [9] R.B. Randall. A history of cepstrum analysis and its application to mechanical problems. In *Conference Surveillance 7*, Chartres, 29-30 October 2013.
- [10] T Fournel, J. Danière, J. Moine, J. Pigeon, M. Courbon, and J.P. Schon. Utilisation du cepstre d'énergie pour la vélocimétrie par images de particules. *Traitement du signal*, 9(3):267 – 271, 1992.
- [11] SAFRAN. Safran contest. In *Conference Surveillance 8*, Roanne, 20-21 October 2015.